J. exp. Biol. 145, 439–454 (1989)
Printed in Great Britain © *The Company of Biologists Limited 1989*

SEPARATION OF HYDROGEN ION CURRENTS IN INTACT MOLLUSCAN NEURONES

BY M. P. MAHAUT-SMITH*

Department of Physiology, Medical School, University Walk, Bristol BS8 1TD

Accepted 12 May 1989

Summary

The amplitude and rate of activation of the voltage-dependent H^+ pathway in intact *Helix* neurones were investigated using standard two-electrode voltage-clamp techniques. Na^+ and K^+ currents were inhibited by a Na^+-free, tetraethylammonium (TEA^+) (low-Cl^-) saline and by use of Cs^+-filled electrodes. Ca^{2+} currents were abolished by holding the membrane at −15 to −10 mV. Depolarizing voltage pulses from these low potentials activated outward currents whose tail current reversal potential shifted with changes in intracellular and extracellular pH, but not with changes in external KCl; thus these remaining currents are carried by hydrogen ions. Furthermore, the amplitude of the voltage-dependent outward current increased as the outward gradient for H^+ was increased and a rise in pHi shifted the activation towards negative potentials. At physiological pH levels, H^+ currents were typically 60 nA at 30 mV (cell diameter 200–250 μm). H^+ currents were rapidly activated; the time to half maximal current at 30 mV was less than 5 ms in the pHi range tested (7·4–6·9) (pHe 7·4). The H^+ pathway will therefore be activated by individual action potentials and may play an important role in pH homeostasis during intense neural activity.

Introduction

The membrane of snail neurones becomes highly permeable to hydrogen ions upon depolarization (Thomas & Meech, 1982). Voltage-activated outward H^+ currents can be detected in internally perfused *Lymnaea* neurones following inhibition of inward currents and removal of K^+ from both sides of the membrane (Byerly *et al.* 1984). The rapid activation and relatively large amplitude of these currents has led to the suggestion that the H^+ pathway compensates for the acidification following Ca^{2+} influx during trains of action potentials and Ca^{2+}/H^+ exchange in the cytoplasm (Ahmed & Connor, 1980). However, the *Lymnaea* study used a high internal buffer concentration and the perfusion technique has been shown rapidly to remove certain cytoplasmic cofactors required for the maintenance of calcium currents (Byerly & Yazejian, 1986). These alterations may

* Present address: Physiological Laboratory, Downing Street, Cambridge CB2 3EG.

Key words: ionic current, pH, hydrogen ion, neurone.

also affect the properties of the H^+ pathway: H^+ currents recorded from intact axolotl oocytes are activated with a time constant that is more than an order of magnitude slower than in the perfused neurone (Barish & Baud, 1984). This may be a species difference or a true reflection of H^+ current kinetics in cells with normal cytoplasm. This study was therefore aimed at isolating H^+ currents in intact *Helix* neurones, where cofactors are not washed out and stable ionic currents can be recorded for many hours.

H^+ currents were found to be present in intact *Helix* neurones bathed in a Na^+-free, TEA^+ saline that were voltage-clamped with Cs^+-filled microelectrodes. Currents carried only by H^+ were studied following inactivation of Ca^{2+} currents at low holding potentials.

Materials and methods

Preparation

The suboesophageal ganglion of *Helix aspersa* was dissected as described previously (Kerkut & Meech, 1966). Experiments were performed on large cells approximately 200–250 μm in diameter. The preparation was continuously perfused at a rate of 5 ml min^{-1}. The bath volume was 0·8–1 ml and solution changes were complete within 40–45 s. All experiments were carried out at room temperature (19–22°C).

Salines

Normal saline contained (in mmol l^{-1}) NaCl, 80; $CaCl_2$, 7; $MgCl_2$, 5; KCl, 4; Hepes, 20, pH 7·4. The $0Na^+$, TEA^+ (low-Cl^-) saline contained (in mmol l^{-1}) TEABr, 80; $CaCl_2$, 7; $MgCl_2$, 5; KCl, 4; Hepes, 20, pH 7·4. In salines used for calibration of the pH microelectrode and in experiments where the external pH was varied, Hepes was used to buffer the solution in the pH range 7·00–7·75 and Pipes was used in the pH range 6–6·75. NaOH was used to adjust pH in normal salines and *N*-methyl glucamine was used in Na^+-free salines.

Chemicals of AnalaR grade were used and came from BDH, except for the following: Hepes, Pipes, *N*-methyl glucamine (Sigma) and tetraethylammonium bromide (Eastman Kodak Co.; reported to be free from the impurity triethylamine, which alkalinizes the cytoplasm, Zucker, 1981).

Microelectrodes

Recessed-tip glass pH electrodes were constructed according to the design of Thomas (1978). All electrodes had responses of at least 55 mV to 1 pH unit change (7·5 to 6·5) that was 90 % complete within 1 min. Voltage electrodes were filled with a solution of 3 mol l^{-1} CsCl and 0·1 mol l^{-1} potassium acetate and had a resistance of 1·5–5 MΩ. The small amount of potassium acetate appeared to reduce the chance of a sudden increase in tip potential. These electrodes were shielded with electrically conductive paint to within 1 mm from the tip and then insulated with nail varnish. The shield was 'driven' from the amplifier headstage.

The current-passing electrode was filled with 3 mol l^{-1} CsCl and had a resistance of 1–4 MΩ. The acid-injection electrode was filled with 1–2 mol l^{-1} HCl and had a resistance of 25–30 MΩ.

Electrical arrangements

The voltage, current and acid-injection electrodes were connected to microelectrode amplifiers (World Precision Instruments, model Ks-700). The current injection system of the WPI amplifier was used to inject acid ionophoretically. Standard two-electrode voltage-clamp techniques were used, similar to those described by Meech & Standen (1975). The output from the clamp was fed through a switch which allowed the system to work in current-clamp or voltage-clamp mode. The voltage command was complete and the capacitative transient over within 300 μs. The resistance in series with the membrane was measured from the initial voltage step observed under current-clamp upon current injection. The measured value was about 6 KΩ and would produce an error of less than 2 mV for the largest currents recorded in these experiments. Clamp current was measured by an amplifier in a virtual earth configuration which was connected to the bath through a 3 mol l^{-1} KCl–agar bridge. The currents were low-pass filtered at a −3 dB frequency of 600 Hz. The output of the pH electrode was connected to a varactor bridge amplifier (311J, Analog Devices). The membrane potential was subtracted from the output of the 311J, using a differential amplifier, to give pHi.

Membrane potential, clamp current, injection current and pHi were continuously monitored on a potentiometric chart recorder. Membrane potential and clamp current during short voltage steps were displayed on a storage oscilloscope and photographed on 35 mm film. The negatives were enlarged and analysed by hand.

Results

Separation of H^+ currents using a Na^+-free, TEA^+ saline

The H^+ pathway in molluscan neurones is activated by membrane depolarization (Thomas & Meech, 1982). To make a full study of H^+ currents under voltage-clamp, currents carried by other ions which are also activated by depolarizing steps must be blocked. Fig. 1A (top trace) shows a typical voltage-clamp record during a brief (60 ms) depolarizing voltage pulse with the cell in normal saline. The membrane potential was stepped from −50 mV to 30 mV which activated an inward current, followed by a sustained outward current. Previous studies have demonstrated that the inward current is carried by both Na^+ and Ca^{2+}, the relative contribution depending on the cell type (Meech & Standen, 1975; Standen, 1975*a*,*b*; Kostyuk & Krishtal, 1977). The outward current is carried mainly by K^+ (Meech & Standen, 1975); at physiological pH levels, the contribution of H^+ is small (Thomas & Meech, 1982; Byerly *et al.* 1984). A third component of the outward current is a small linear current which corresponds to the resting membrane resistance of 1·5–5 MΩ (termed the leakage current).

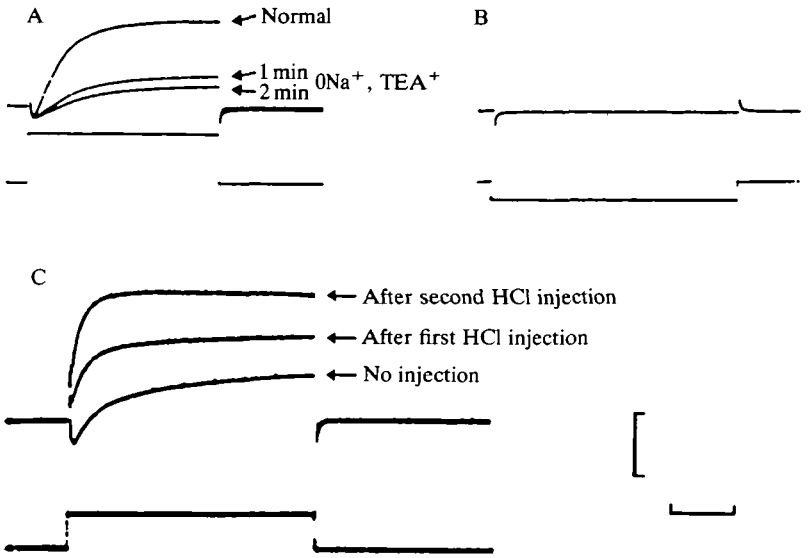

Fig. 1. Effect of $0Na^+$, TEA^+ saline and intracellular acid injection on voltage-clamp currents. Upper records are current and lower records are voltage. (A) Superimposed records for an 80 mV depolarizing step taken in normal saline and after 1 and 2 min of exposure to $0Na^+$, TEA^+ saline. (B) Example of the record for a 30 mV hyperpolarizing voltage step used for determination of leakage current. (C) Superimposed records from a cell in $0Na^+$, TEA^+ saline for a 60 mV depolarizing voltage step before and after two acid injections of 40 nA for 30 s. Scale bars: Vertical: voltage, 100 mV; current, A 400 nA, B 100 nA, C 50 nA. Horizontal: A,C 20 ms, B 40 ms. Holding potential: A,B −50 mV, C −40 mV.

Hyperpolarizing voltage pulses activated no voltage-dependent currents, as shown in Fig. 1B. The current record contained only capacitative and inward leakage components, and was used to correct for the leak current in current–voltage relationships.

TEA^+ is an effective blocker of both voltage- and Ca^{2+}-activated K^+ channels in these cells (Meech & Standen, 1975), whereas H^+ currents are relatively resistant to TEA^+ (Byerly *et al.* 1984), so a $0Na^+$, TEA^+ saline was used in the present study. The fast inactivating K^+ current (I_A) was inactivated by holding the cell at, or more depolarized than, −55 mV (Neher, 1971). In a further attempt to reduce K^+ currents, the voltage-clamp electrodes were filled with CsCl, which will leak into the cytoplasm. Cs^+ has a low permeability through K^+ channels and blocks K^+ currents in a number of preparations (see Latorre & Miller, 1983; Cook, 1988).

The $0Na^+$, TEA^+ saline caused a large reduction in the net outward current (Fig. 1A). The relative amounts of inward and outward currents remaining in cells in the modified saline depended on both the cell type and the amplitude of the depolarizing pulse. The current was mainly inward when the cell was stepped from near the normal resting potential to less than 0 to +10 mV (see current–voltage

relationship in Fig. 2B). At larger positive potentials, the outward current increased and overlapped with the inward current (as in Fig. 1A, lower trace). Under these conditions, the inward current is carried by Ca^{2+} and the outward current may be a combination of remaining K^+ currents and H^+ current.

Injection of HCl into cells exposed to the modified saline increased the size of the voltage-dependent outward current. Fig. 1C shows the currents recorded during an 80 ms pulse to 20 mV (holding potential −40 mV), in the $0Na^+$, TEA^+ saline and after two consecutive injections of HCl. The currents in the hyperpolarizing direction were identical throughout (not shown), indicating no change of leak current. The outward current induced by acid injection was often large and sufficiently rapidly activated to obscure the Ca^{2+} current, even at low positive potentials.

In many cell types, a reduced pHi blocks Ca^{2+} and K^+ currents (see Moody, 1984, for a review). However, the increased driving force for H^+ would tend to increase H^+ currents as shown for perfused *Lymnaea* cells (Byerly *et al.* 1984). The following experiments investigate the nature of the outward current in the $0Na^+$, TEA^+ saline and show that the outward current increases following acid injection because of an enhanced H^+ current.

To study the outward current in the modified saline in more detail, it was essential to block the Ca^{2+} current. Three different techniques for inhibiting Ca^{2+} currents were investigated; removal of external Ca^{2+}, block by internal H^+ and inactivation by low holding potentials.

Removal of external Ca^{2+} was not successful as a method of abolishing Ca^{2+} currents for two reasons. First, exposure to $0Ca^{2+}$ (Mg^{2+}), $0Na^+$, TEA^+ saline, resulted in a large increase in leak conductance in most cells. Second, in the few cells that withstood this treatment, some Ca^{2+} must have remained in the bath, since inward currents still remained after 10–15 min perfusion with Ca^{2+}-free saline.

Ca^{2+} currents are irreversibly blocked by a decrease in pHi (see Byerly *et al.* 1984; Byerly & Moody, 1986). To lower pHi, the following protocol was used. H^+ was injected into the cell by ionophoresis and, after a few minutes at low pHi, the membrane was held at 0 mV. At this potential, the H^+ pathway opens, resulting in H^+ efflux (Thomas & Meech, 1982) and pHi recovers to near 7·4. This reversed the acid-induced rise in outward current (see later). The effect of cytoplasmic acidification on the Ca^{2+} current was measured after Ca^{2+} channels had recovered from inactivation at 0 mV. Ca^{2+} currents in *Helix* were blocked by injections of acid; however, significant inward currents remained following 2–3 min of exposure to the lowest pHi that cells tolerated (about 6·0).

Use of low holding potentials to inactivate Ca^{2+} currents

The third method of blocking Ca^{2+} currents was to reduce the cell membrane holding potential, which can totally inactivate Ca^{2+} channels in *Helix* (Standen, 1975*b*). A low holding potential can be used in a study of the H^+ pathway because

H^+ currents show little or no voltage-dependent inactivation (Thomas & Meech, 1982; Byerly *et al.* 1984).

Following successful impalement by voltage-, current- and pH-sensitive microelectrodes, the membrane potential was clamped at −50 mV (Fig. 2A). pHi initially rose as the cell recovered from an acid load incurred during impalement. Exposure to $0Na^+$, TEA^+ saline caused pHi to fall, presumably because the normal pHi-regulating mechanism is blocked in Na^+-free salines (see Thomas, 1984, for a review). When the holding potential was depolarized to −30 mV, and subsequently to −15 mV, pHi was further reduced. The pH change was slowed in

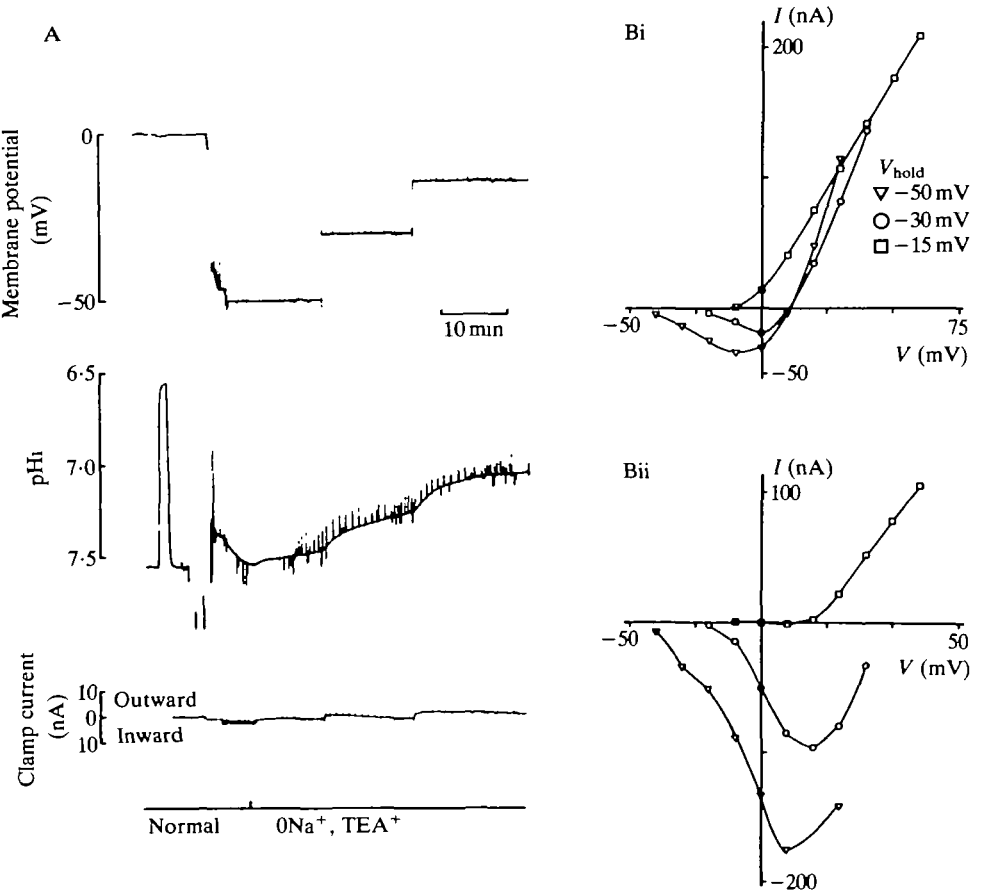

Fig. 2. (A) Effect of holding potential on pHi. Continuous chart recording of membrane potential, pHi and clamp holding current. Holding potentials were −50, −30 and −15 mV. Transients from 60 ms voltage-clamp steps were attenuated by the recorder. (B) Leak-corrected current-voltage relationships for peak outward (i) and peak inward currents (ii) at three holding potentials. Abscissa: membrane potential. Ordinate: (upper graph) current at 60 ms; (lower graph) peak inward current or smallest outward current. Measurements taken from 60 ms pulses at −50 mV (▽) just before depolarizing to −30 mV; after 10 min at −30 mV (○); and after 10 min at −15 mV (□). Curves drawn by eye.

nominally Ca^{2+}-free saline and may therefore be due to Ca^{2+} influx through voltage-dependent Ca^{2+} channels. The acidification arises from Ca^{2+}/H^+ exchange in the cytoplasm (Meech & Thomas, 1977; Ahmed & Connor, 1980).

Throughout the experiment of Fig. 2A, voltage-dependent currents were measured during 60 ms voltage steps. The leak-subtracted current–voltage relationships at −50 mV, −30 mV and −15 mV, after approximately 10 min at each potential, are plotted in Fig. 2B. Fig. 2Bi shows the current at 60 ms and Fig. 2Bii shows the peak inward or smallest outward current. The inward current was inhibited at all potentials by a reduced holding potential and no inward current was activated by depolarizing pulses from −15 mV. The net outward current was slightly decreased by changing the holding potential from −50 to −30 mV, but then generally increased (in the potential range studied) by further depolarizing to −15 mV. It is difficult to assess the absolute changes in currents carried by individual ionic species owing to the number of ions involved. However, the results are consistent with the development of H^+ current as pHi falls, and a decrease in Ca^{2+} current (and residual K^+ current) with inactivation due to the low holding potential and acidification of the cytoplasm. The protocol described above, approximately 10–15 min at a holding potential of −30 mV followed by a further reduction in potential to −15 or −10 mV, was tested in at least 15 cells and found to inactivate all inward current in the $0Na^+$, TEA^+ saline. The remaining outward current could be carried by H^+, through the voltage-gated H^+ pathway or by K^+, through unblocked K^+ channels. The following experiments investigate the nature of this outward current.

Effect of changing external potassium concentration on tail currents following outward currents at low holding potentials

Fig. 3A shows tail currents at −5 and −25 mV following 60 ms pulses to 55 mV from a holding potential of −15 mV, for three levels of external K^+. Tail current amplitude was measured as the difference between the current at 6 ms (after the capacitative current) and the holding current, measured about 100 ms after the pulse. This method eliminated the difference in the size of the leak component, which varied with the external K^+ concentration. It was also the method used to measure H^+ tail currents by Byerly *et al.* (1984) in internally perfused *Lymnaea* neurones.

The tail currents at 6 ms in different levels of K^+ are plotted as a function of membrane potential in Fig. 3B. The reversal potential was −23 mV and was not shifted by changes in external $[K^+]$ (confirmed in five other cells). Following pulses to more positive potentials, in a solution of 20 mmol l^{-1} K^+, the tail current reversal potential was sometimes, but not always, shifted to more negative potentials (data not shown). The largest shift observed was 6 mV (0 mmol l^{-1} K^+ to 20 mmol l^{-1} K^+), following a 100 ms pulse to 65 mV from a holding potential of −15 mV. This suggests that K^+ does not contribute to the outward currents activated by depolarizing voltage steps up to 55 mV from low holding potentials in the modified saline.

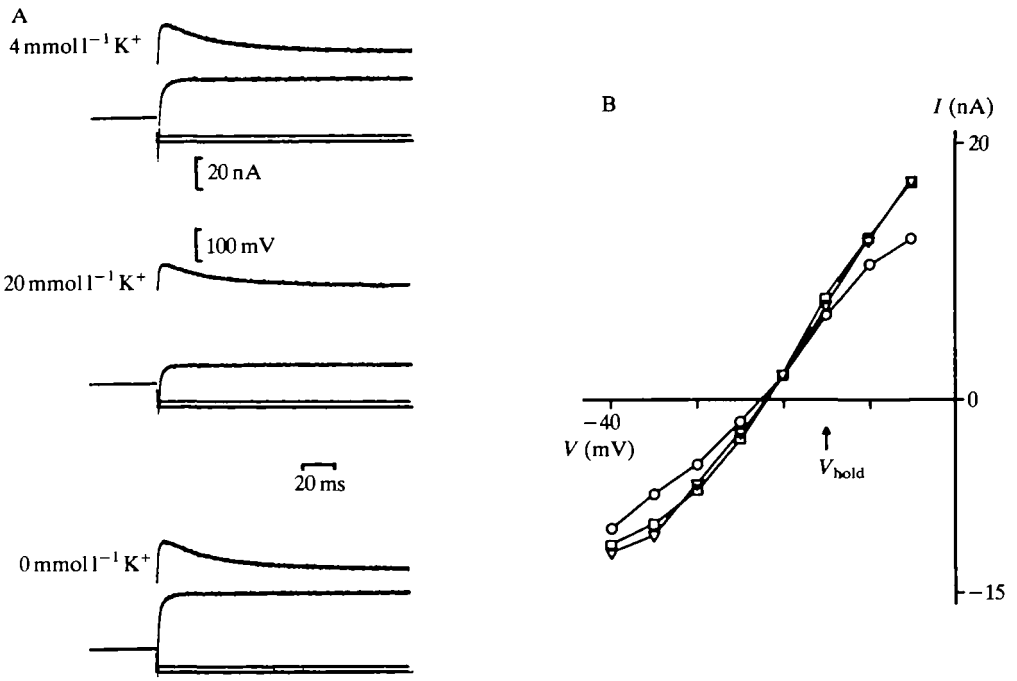

Fig. 3. Effect of changing external potassium concentration on the tail currents. (A) Tail current (upper) and voltage (lower) records on return to −5 and −25 mV following a 60 ms pulse to 55 mV (holding potential −15 mV). (B) Plot of tail current amplitude on return to various potentials. Ordinate: tail current at 6 ms. Abscissa: membrane potential. ▽, 4 mmol l^{-1} K^+; ○, 20 mmol l^{-1} K^+; □, K^+-free saline. Points joined by straight lines. pHi: 7·03 ($4K^+$); 7·05 ($20K^+$); 7·02 ($0K^+$): pHe: 7·49 ($4K^+$); 7·52 ($20K^+$); 7·47 ($0K^+$).

Effect of pHi on outward currents

The effect of changing intracellular pH was tested in cells clamped at low holding potentials to reduce Ca^{2+} currents and Ca^{2+}-activated currents as described above. To vary pHi, the cytoplasm was acidified by injecting acid and realkalinized by holding the membrane at 0 to +20 mV, which activates the H^+ pathway, as described earlier. At each pH level, the cell was held at −10 mV and ionic currents were measured in response to voltage steps of 80 ms in 10 mV increments up to +50 mV. Superimposed traces of current are shown in Fig. 4A for one acidic and one alkaline pH level. At the right of the figure, tail currents are shown following an 80 ms pulse to +50 mV. Superimposed traces are shown, each during repolarization to the indicated potential. The leak-corrected current amplitude, and tail currents, measured as described earlier, are plotted as a function of membrane potential in Fig. 4B,C. At more acidic levels of pHi, the amplitude of the voltage-activated currents was increased and the tail current reversal potential shifted to more negative potentials. E_{rev} shifted by -23 ± 5 mV (S.D., $N = 6$) per pH unit over the pH range 6·5–7·45. The reversal potential of a

H^+-selective current would be expected to shift 58 mV for every unit shift in pHi. The possible explanations for the smaller shift reported here are fully discussed below.

In cells held at these low potentials, successive voltage pulses, each 60 ms long, could be applied with intervals as short as 2–3 s without a reduction in current amplitude. This suggests that the voltage-activated current shows little voltage-dependent inactivation. Previous studies have reported that H^+ currents and the H^+ pathway are not inactivated during depolarizing steps (Thomas & Meech, 1982; Byerly *et al.* 1984; Barish & Baud, 1984). K^+ currents, in contrast, display marked inactivation during short voltage steps.

Even in the absence of voltage pulses, with the membrane held at −10 mV, the

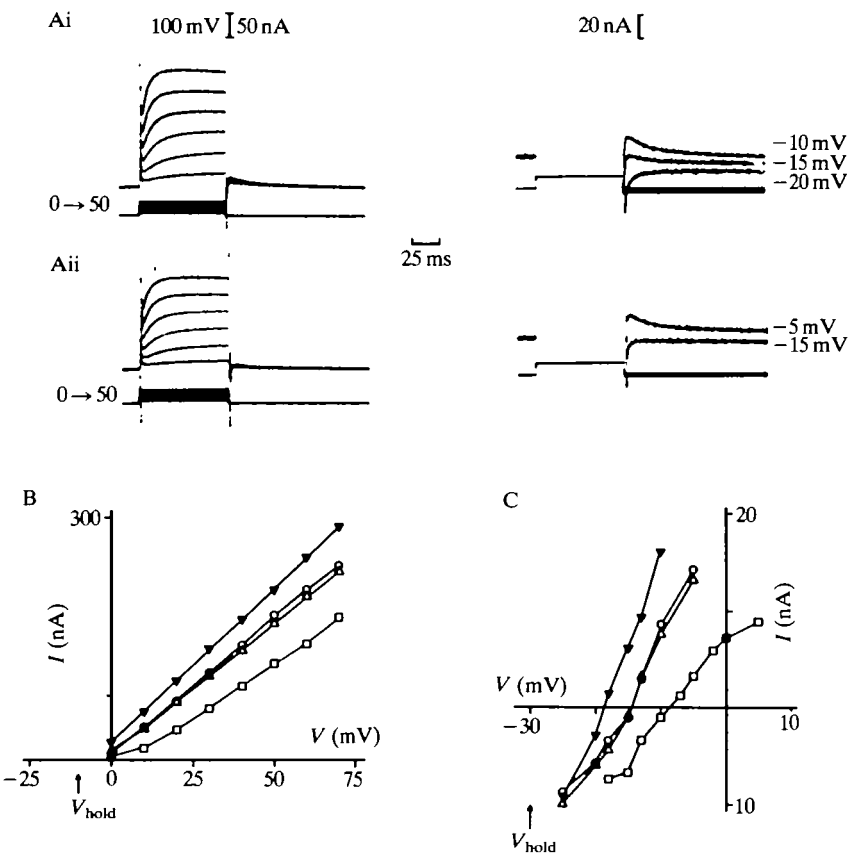

Fig. 4. Effect of pHi on membrane currents. Holding potential, −10 mV. (A) Records shown at pHi 6·99–6·96 after acid injection (Ai); and at pHi 7·22–7·19 after a period of holding at +15 mV to allow acid efflux (Aii). Traces on the left are for 80 ms pulses in 10 mV steps to the potentials indicated. Records on the right followed 80 ms pulses to 50 mV, returning to the potentials indicated. (B,C) Leak-corrected current–voltage relationships. Effect of pHi on voltage-activated current (B) and tail currents (C). Straight lines are drawn between the points. ▼, pHi 6·99–6·96; ○, pHi 7·21–7·17; □, pHi 7·52–7·44; △, pHi 7·22–7·19.

measured pHi slowly changed at most pHi levels. Following an acid injection, pHi increased, owing to efflux through the H^+ pathway; this rise in pHi was stopped by hyperpolarizing the membrane to −60 mV. Following a period at 0 to +20 mV, pHi slowly decreased. This can be explained by an influx of H^+, drawn down its electrochemical gradient into the cell, that does not regulate its pHi in these salines. As a result of these pHi changes, the current amplitudes and tail currents were often measured over a narrow range of pHi values which are indicated in Fig. 4.

The rate of activation of the voltage-dependent current was measured by the time to half maximum current ($t_{1/2}$). Activation increased with the size of the depolarizing pulse; typically $t_{1/2}$ decreased from 15 ms at 0 mV to 2·5 ms at 40 mV. The degree to which activation was dependent on pHi varied in different cells. In a few cells, $t_{1/2}$ at potentials up to +30 mV was increased as the cytoplasm was acidified. In most cells, however, $t_{1/2}$ was not significantly affected by lowering pHi. In all cases, the activation kinetics upon depolarizing to potentials in the range 40–50 mV remained constant as pHi was varied.

Conductance

To detect shifts in the potential-dependence of activation, chord conductances were calculated to allow for the driving force and to provide an estimate of the degree of activation of the H^+ pathway. The measured reversal potential for pulses to 30 or 40 mV was used as these were below the potential at which E_{rev} was affected by the external K^+ concentration (see above).

The steady-state conductance (G) at each potential (V) can be described by the following equation:

$$G(V) = G_{max}/[1 + \exp \frac{-zF}{RT}(V_{1/2} - V_m)] , \quad (1)$$

where z is the effective charge on the gating particle, G_{max} is the maximum conductance, F is Faraday's constant, R is the gas constant, T is absolute temperature, V_m is the potential during the voltage step and $V_{1/2}$ is the voltage of half-maximum conductance.

At 22°C, F/RT has a value of 39 V^{-1}. zF/RT is a constant that describes the voltage-dependence of the pathway. Equation 1 was rearranged to give:

$$\ln \left(\frac{G}{G_{max} - G}\right) = \frac{zF}{RT}(V_{1/2} - V_m) . \quad (2)$$

$\ln(G/G_{max} - G)$ is plotted as a function of the membrane potential in Fig. 5A for two cells which were held at −10 mV and in which pHi was approximately 6·9. The relationship is linear with a gradient of zF/RT and intercepts the ordinate at $V_{1/2}$ (3 mV). The slope was e-fold change in conductance per 14 mV, which gives a gating charge of 2. Values for z and $V_{1/2}$, calculated in this way, were used in equation 1 to provide the sigmoidal curves for the conductance–voltage relationships. Conductance–voltage relationships for the currents shown in Fig. 4B are

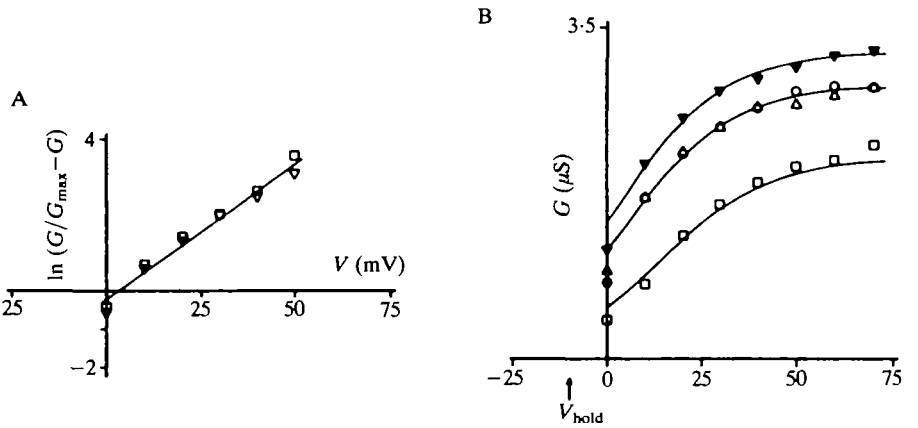

Fig. 5. pHi and membrane conductance. (A) Measurement of conductance. Data from two cells with similar tail current reversal potential (▽, −19 mV; □, −20 mV). Ordinate, $\ln(G/G_{max}-G)$ (see text for explanation). Abscissa, membrane potential. Line drawn by eye. Intercept with ordinate is $V_{1/2} = 3$ mV. Slope of line is e-fold change in conductance per 14 mV. (B) Conductance–voltage relationships (data from cell shown in Fig. 4). Ordinate, conductance calculated from equation 1 as described in text. Abscissa, membrane potential. Solid lines drawn using equation 2, as described in text using values for $V_{1/2}$ and slope that were obtained from graphs such as that in A. Holding potential, −10 mV. ▼, pHi 6·99–6·96; ○, pHi 7·21–7·17; □, pHi 7·52–7·44; △, pHi 7·22–7·19.

plotted in Fig. 5B. A fall in pHi increased the conductances at all potentials and produced a negative shift in the voltage at which conductance was half maximal. The average shift in $V_{1/2}$ was −23 mV per pH unit ($N = 5$) in the pH range 6·5–7·5.

Effect of changing pHe

Fig. 6A shows the effect of changing pHe on the outward current activated by 50 mV pulses from a holding potential of −15 mV and shows the tail currents on return to three potentials, −10, −15 and −20 mV. The complete leak-corrected current–voltage relationships at three different pHe values are plotted for the voltage-dependent current in Fig. 6B and for the tail currents in Fig. 6C. As the concentration of H^+ in the bathing solution was increased, the amplitude of the outward current was reduced and the tail reversal potential shifted towards positive potentials. In four cells, the average shift in E_{rev} was 20 ± 3·6 mV (S.D.) per pHe unit change. A change in pHe also caused pHi to drift slowly in the same direction; for example, in the cell shown in Fig. 6, the currents were measured at pHi 7·30–7·28 in pH 7·7 saline, at pHi 7·18–7·17 in pH 7·01 saline and at pHi 7·09–7·06 in pH 6·75 saline. The average drift in pHi was 0·3 pH unit ($N = 4$) per unit change in pHe. Therefore, the average shift in E_{rev}, corrected for the change in H^+ gradient, is 29 mV per pH unit. These pH shifts and their effects on measurement of E_{rev} are discussed below.

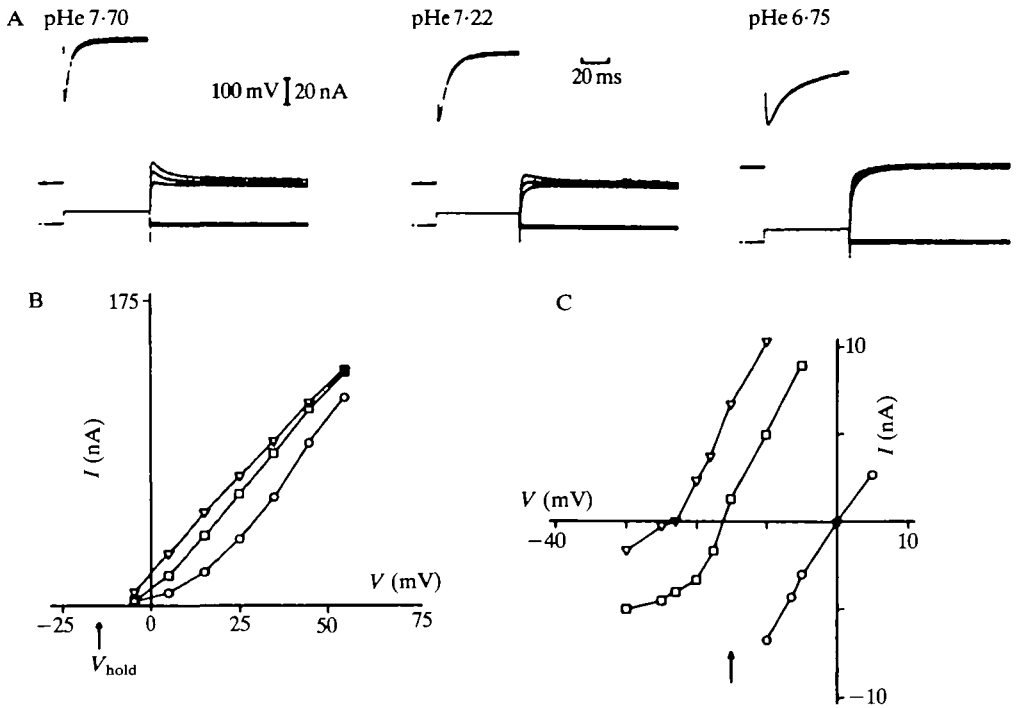

Fig. 6. Effect of pHe on membrane currents. (A) Current (upper) and voltage (lower) records at three extracellular pH levels. Holding potential, −15 mV; pulse to +35 mV. Three records are superimposed at each pH, returning to −10, −15 and −20 mV. (B,C) Leak-corrected current–voltage relationships. (B) Voltage-activated current and (C) tail current. Data shown for pHe 7·70 (▽); pHe 7·22 (□) and pHe 6·75 (○). Straight lines are drawn between the points.

Discussion

To assess the amplitude and kinetics of H^+ efflux through the H^+ pathway under physiological conditions, H^+ currents must be separated from other ionic currents using conditions where the buffering power and cytoplasmic constituents remain relatively undisturbed. In this study intact *Helix* neurones were exposed to a $0Na^+$, TEA^+ (low-Cl^-) saline and voltage-clamped with Cs^+-filled microelectrodes. These cells displayed inward currents and small outward currents in response to depolarizing voltage pulses. The inward current is carried by Ca^{2+} and was abolished by holding the cell membrane at a low holding potential (−15 or −10 mV). The evidence that, under these conditions, the residual voltage-dependent outward currents were largely carried by H^+ can be summarized as follows.

1. The tail current reversal potential shifted with changes in pHi and pHe in the direction expected for the change of hydrogen ion equilibrium potential. Changes in external potassium had no effect on the reversal potential following small depolarizations.

2. The amplitude of the voltage-activated current depended on pHi and pHe, such that an increased outward driving force for H^+ resulted in a larger outward current.

3. A reduction of pHi increased the maximum conductance and shifted the conductance–voltage relationship in the negative direction along the voltage axis.

4. Divalent cations, such as Cd^{2+} and Zn^{2+}, which block the H^+ pathway and H^+ currents in molluscan neurones (Thomas & Meech, 1982; Byerly *et al.* 1984; Meech & Thomas, 1987), also blocked the residual outward currents in the $0Na^+$, TEA^+ saline (Mahaut-Smith, 1987, 1989). The voltage-dependent K^+ current, which is the most likely current to remain under these conditions, is not blocked by these agents in *Helix* (Meech & Standen, 1975; M. P. Mahaut-Smith, unpublished observations).

5. The residual current showed little or no voltage-dependent inactivation. Successive short pulses could be administered as close as 2–3 s apart without significant attenuation of the outward current. The H^+ pathway does not inactivate (Thomas & Meech, 1982), whereas Ca^{2+}- (and, as a consequence, Ca^{2+}-activated currents) and voltage-activated K^+ currents in molluscan neurones require intervals of much longer duration (20–30 s) to recover from inactivation (Kostyuk *et al.* 1975; Plant & Standen, 1981; M. P. Mahaut-Smith, unpublished observations).

The shifts in tail current reversal potential observed with pH in this study (approximately 29 mV for a shift in pHe and 24 mV for a shift in pHi) are closer to the value expected if the H^+ pathway channel were to transport H^+ (or OH^-) as a doubly charged species. If H^+ does in fact pass through the H^+ pathway in the monovalent ionic form, other explanations must be considered for the deviation from the theoretical value of 58 mV shift in E_{rev} per pH unit. Other ionic species could contribute to the tail current, although an alteration in K^+ concentration was without effect, at least for depolarizations of small amplitude. Na^+ could carry a current out of the cell, but it is likely that, in the Na^+-free medium, the internal Na^+ concentration falls to very low levels. There is no cytosolic sink for Na^+, so any Na^+ component would rapidly diminish with successive pulses, which was not observed: the outward current was stable over an entire experiment, during which many depolarizing pulses were applied. Another possible explanation for the low shift in E_{rev} with pH is that the pH at the membrane surface is different from the pH in the bulk phase, such that the local H^+ gradient is reduced. This is particularly relevant in these experiments where the measured pHi slowly changed under most conditions. When the gradient for H^+ was outward, after an injection of acid, this was due to H^+ efflux through the H^+ pathway and pHi increased. When the H^+ gradient was reversed, after returning from a depolarized potential, or during exposure to acidic salines, pHi slowly decreased, presumably owing to H^+ leaking into the cell, which does not regulate its pHi in Na^+-free salines. pHi was only stable when the H^+ equilibrium potential was close to the holding potential (-15 or -10 mV).

In Fig. 7, the measured reversal potential is plotted as a function of the

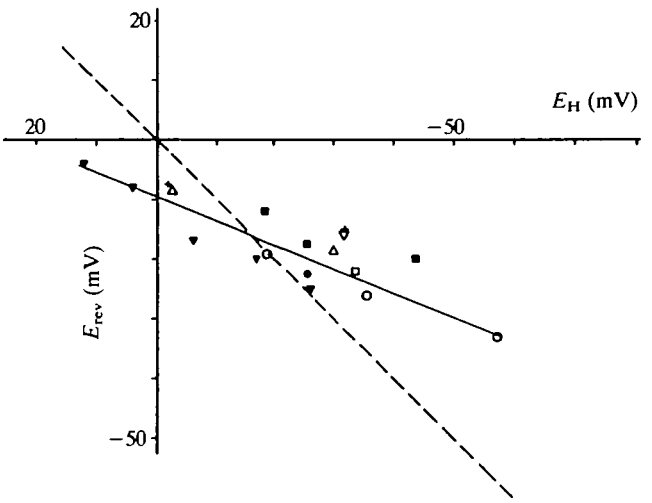

Fig. 7. Comparison of E_H and E_{rev}. Ordinate, tail current reversal potential. Abscissa, hydrogen ion equilibrium potential calculated from the pH measurements in the bulk phase. The dashed line represents the relationship predicted from the Nernst equation for movement of H^+. The continuous line was drawn by eye through the experimental points. Each symbol represents data from a single cell.

hydrogen ion equilibrium potential. E_{rev} is only close to E_H when E_H is near the holding potential. At other values, E_{rev} underestimates the H^+ gradient, which can be explained by the constant movements of H^+ described above. In conclusion, the low shift in E_{rev} with the measured internal and external pH is due, at least in part, to a reduction in H^+ gradient at the membrane surface, which is caused by a constant movement of H^+ under the conditions used in these experiments.

These results suggest that a component of the voltage-activated outward current in cells perfused with normal saline will be carried by H^+. At normal pHi levels (approximately 7·3–7·4), H^+ currents in *Helix* neurones were typically about 60 nA at 30 mV, but they are probably slightly larger in normal saline owing to the small inhibitory action of TEA^+ on the H^+ pathway (Byerly *et al.* 1984; Meech & Thomas, 1987). At acidic pHi levels, the H^+ current significantly increases; at 30 mV, currents in *Helix* approximately doubled in amplitude on reducing pHi from 7·19 to 6·53. However, this still represents only a small proportion of the normal steady-state outward current in these cells, measured at more than 3 μA at 30 mV in cell A (Meech & Standen, 1975). The contribution of H^+ currents may be significant at shorter times because of the rapid activation of the H^+ pathway.

Inward currents in molluscan neurones are of the same order of magnitude as H^+ currents. This study (for example Fig. 1C) demonstrates that H^+ currents can contaminate Ca^{2+} currents measured under voltage-clamp when the cytoplasm acidifies. Cytoplasmic acidosis can arise under experimental conditions that block

pHi regulation, such as in the Na^+-free salines used in this study. Under these conditions, the amplitude and kinetics of both inward and outward currents must be carefully examined for the presence of H^+ currents. Byerly & Moody (1986) describe the significant contribution of H^+ currents to voltage-dependent currents in *Lymnaea* neurones internally perfused with low pHi solutions.

Comparison with Lymnaea *neurones*

At pHi 7·3 (pHe 7·4), Byerly *et al.* (1984) recorded H^+ currents of about 15 nA at 30 mV in *Lymnaea* neurones of 100 μm diameter. The *Helix* cells used in this study had diameters of about 200 μm which, assuming the cells to be simple spheres, represents approximately four times the surface area. When this difference is taken into account, H^+ currents recorded in the two preparations were of similar amplitude. The rate of activation of H^+ currents is also comparable in both preparations; the time to half-maximum current at 30 mV when pHe was 7·4 and pHi was approximately 7·3 or more acidic, was always less than 5 ms in both preparations. This implies that the technique of intracellular perfusion does not remove any cofactors which may be required for the H^+ pathway to function. It also suggests that the currents observed in perfused neurones are not simply a function of the high concentration of pH buffers used.

Unique property of H^+ currents: proposed function

An unusual property of the H^+ pathway is that the conductance–voltage relationship shifts along the voltage axis in the negative direction when internal $[H^+]$ increases. This may reflect its role in pHi regulation; as the cytoplasm is acidified, the conductance rises to increase the efflux of protons and restore pHi.

Thomas & Meech (1982) and Byerly *et al.* (1984) have suggested that the H^+ pathway may compensate for the intracellular acid load which occurs during trains of action potentials (Ahmed & Connor, 1980). In cell A of *Helix*, the action potential reaches nearly 40 mV in amplitude and has a duration of approximately 3–4 ms at 30 mV (Standen, 1975*a*). The rapid activation of H^+ currents shown in this study and in perfused *Lymnaea* neurones (Byerly *et al.* 1984) certainly suggests that the H^+ pathway opens and releases H^+ from the cell during individual action potentials. The H^+ pathway could be functionally more important if it occurs in cells where the action potential has a long plateau and where a maintained Ca^{2+} influx occurs, for example in ventricular myocytes. However, it remains to be tested in any cell whether the H^+ pathway actually contributes significantly to pHi regulation or possibly to action potential repolarization under physiological conditions.

I am grateful to Dr R. W. Meech for guidance during these studies and to Professor R. C. Thomas for allowing me to use his laboratory to make pH electrodes. Thanks also to Dr R. W. Meech and Dr M. G. Evans for comments on the manuscript and Michael Rickard for expert technical assistance. The work was supported by the Medical Research Council.

References

AHMED, Z. & CONNOR, J. A. (1980). Intracellular pH changes induced by calcium influx during electrical activity in molluscan neurones. *J. gen. Physiol.* **75**, 403–426.

BARISH, M. E. & BAUD, C. (1984). A voltage-gated hydrogen ion current in the oocyte membrane of the axolotl, *Ambystoma*. *J. Physiol., Lond.* **352**, 243–263.

BYERLY, L., MEECH, R. W. & MOODY, W., JR (1984). Rapidly activating hydrogen ion currents in perfused neurones of the snail, *Lymnaea stagnalis*. *J. Physiol., Lond.* **351**, 199–216.

BYERLY, L. & MOODY, W. J. (1986). Membrane currents of internally perfused neurones of the snail, *Lymnaea stagnalis*, at low intracellular pH. *J. Physiol., Lond.* **376**, 477–491.

BYERLY, L. & YAZEJIAN, B. (1986). Intracellular factors for the maintenance of calcium currents in perfused neurones from the snail, *Lymnaea stagnalis*. *J. Physiol., Lond.* **370**, 631–650.

COOK, N. (1988). The pharmacology of potassium channels and their therapeutic potential. *Trends Pharm. Sci.* **9**, 21–28.

KERKUT, G. A. & MEECH, R. W. (1966). The internal chloride concentration of H and D cells in the snail brain. *Comp. Biochem. Physiol.* **19**, 819–832.

KOSTYUK, P. G. & KRISHTAL, O. A. (1977). Separation of sodium and calcium currents in the somatic membrane of mollusc neurones. *J. Physiol., Lond.* **270**, 545–568.

KOSTYUK, P. G., KRISHTAL, O. A. & DOROSHENKO, P. A. (1975). Outward currents in isolated snail neurones. I. Inactivation kinetics. *Comp. Biochem. Physiol.* **51**C, 359–363.

LATORRE, R. & MILLER, C. (1983). Conduction and selectivity in potassium channels. *J. Membr. Biol.* **71**, 11–30.

MAHAUT-SMITH, M. (1987). The effect of zinc on calcium and hydrogen ion currents in snail neurones. *J. Physiol., Lond.* **382**, 129P.

MAHAUT-SMITH, M. P. (1989). The effects of zinc on calcium and hydrogen ion currents in intact snail neurones. *J. exp. Biol.* **145**, 455–464.

MEECH, R. W. & STANDEN, N. B. (1975). Potassium activation in *Helix aspersa* neurones under voltage clamp: A component mediated by calcium influx. *J. Physiol., Lond.* **249**, 211–239.

MEECH, R. W. & THOMAS, R. C. (1977). The effect of calcium injection on the intracellular sodium and pH of snail neurones. *J. Physiol., Lond.* **265**, 867–879.

MEECH, R. W. & THOMAS, R. C. (1987). Voltage-dependent intracellular pH in *Helix aspersa* neurones. *J. Physiol., Lond.* **390**, 433–452.

MOODY, W. J. (1984). Effects of intracellular H^+ on the electrical properties of excitable cells. *A. Rev. Neurosci.* **7**, 257–278.

NEHER, E. (1971). Two fast transient current components during voltage clamp on snail neurons. *J. gen. Physiol.* **58**, 36–53.

PLANT, T. D. & STANDEN, N. B. (1981). Calcium current inactivation in identified neurones of *Helix aspersa*. *J. Physiol., Lond.* **321**, 273–285.

STANDEN, N. B. (1975*a*). Calcium and sodium ions as charge carriers in the action potential of an identified snail neurone. *J. Physiol., Lond.* **249**, 241–252.

STANDEN, N. B. (1975*b*). Voltage-clamp studies of the calcium inward current in an identified snail neurone: comparison with the sodium inward current. *J. Physiol., Lond.* **249**, 253–268.

THOMAS, R. C. (1978). *Ion-Sensitive Intracellular Microelectrodes: How to Make and Use Them.* London: Academic Press.

THOMAS, R. C. (1984). Review Lecture. Experimental displacement of intracellular pH and the mechanism of its subsequent recovery. *J. Physiol., Lond.* **354**, 3P–22P.

THOMAS, R. C. & MEECH, R. W. (1982). Hydrogen ion currents and intracellular pH in depolarized voltage-clamped snail neurones. *Nature, Lond.* **299**, 826–828.

ZUCKER, R. S. (1981). Tetraethylammonium contains an impurity which alkalizes cytoplasm and reduces calcium buffering in neurones. *Brain Res.* **208**, 473–478.